Catalytic Mechanism of Dihydrofolate Reductase Enzyme. A Combined Quantum-Mechanical/Molecular-Mechanical Characterization of the N5 Protonation Step

Silvia Ferrer, Estanislao Silla, and Iñaki Tuñón*

Departament de Química Física; Universidad de Valencia, 46100 Burjassot, Valencia, Spain

Sergio Martí and Vicent Moliner*

Departament de Ciències Experimentals, Universitat Jaume I, 12071 Castelló, Spain

Received: May 28, 2003; In Final Form: September 22, 2003

The catalytic mechanism of dihydrofolate reductase (DHFR) requires the addition of both a proton and a hydride ion. In *Escherichia coli* dihydrofolate reductase (ecDHFR) Asp27 is considered as the only group in the active site capable of providing the proton for the reduction of the N5−C6 bond, although it is not clear enough if it takes place directly or through a series of water molecules. In this paper we present a theoretical study of the protonation of N5 of the hydrofolate, the prior step of the hydride transfer in dihydrofolate reductase. Hybrid quantum-mechanical/molecular-mechanical (QM/MM) calculations involving a flexible active-site region are used in combination with GRACE software. Two different reaction paths have been found to be feasible. The proposed mechanisms are in agreement with the ordered structure of the X-ray crystallographic water molecules supporting the hypothesis of an indirect proton transfer from Asp27 residue to the N5 atom of the substrate. Asp27 is found to play an important role stabilizing the cationic pteridine ring.

Introduction

Dihydrofolate reductase (5,6,7,8-tetrahydrofolate, NADP oxidoreductase, E.C. 1.5.1.3) catalyses the NADPH-dependent reduction of 7,8-dihydrofolate (DHF) to 5,6,7,8-tetrahydrofolate (THF) in both bacterial and vertebrate cells. This enzyme is necessary for maintaining intracellular pools of THF and its derivatives, which are essential cofactors in the biosynthesis of several amino acids. This property has made DHFR a clinical target for antitumor and antiinfective therapy, and numerous inhibitors have been described.[1,2] Nevertheless, the details of the enzyme molecular reaction mechanism are still unclear and can only be hypothesised at present.[3,4]

The mechanism of the reaction requires the addition of both a proton and a hydride ion. In *E. coli* dihydrofolate reductase (ecDHFR) Asp27 is considered as the only residue in the active site region capable of providing the proton for the reduction of the N5−C6 bond,[5] although it is not clear enough if it takes place directly or through a series of water molecules.[6] In fact, mutation of this residue to a less acidic one (asparagine or serine) results in greatly diminished activity toward dihydrofolate at pH 7, but comparable activity to native DHFR at pH values sufficiently low to protonate dihydrofolate in solution.[5] The presence of a solvent channel with a series of ordered water molecules hydrogen-bonded to the substrate and the protein, and the fact that Asp 27 was too far from the N5 (the proton acceptor atom) support the hypothesis of an indirect protonation to occur. Nevertheless, because various mechanisms for this proton shuttling between Asp27 and N5 have been proposed,[4,7−11] and as a substrate binding role has also been conferred to the Asp 27 residue,[12] further studies are merits to clarify this regard. In fact, a recent contribution of Cummins et al.[4b] focused on the study of the effect of the the protonated/unprotonated state of Asp27 on the hydride transfer step of DHFR arrived to the conclusion that although ab initio and DFT gas phase cluster calculations suggested that the reduction took place when Asp27 was protonated, the same conclusions could not be drawn from hybrid PM3/molecular mechanical force fields plus MD model calculations. It is generally accepted that the protonation of the 7,8-dihydropteridine ring precedes hydride ion transfer and activates the substrate,[13−16] thus being a chemical reaction strongly pH dependent.[6]

It is important to stress on the importance of the inclusion of environment effects to obtain a correct description of the process, not only from a quantitative point of view but also from a qualitative perspective. Hybrid quantum-mechanical/molecular-mechanical (QM/MM) methods provide a powerful way to deal with chemical reactions in very large systems. In these methods, only a small portion of the system is described using quantum mechanics, whereas for the remaining (typically several thousands of atoms) a molecular mechanics force field is employed. The exact characterization of molecular mechanisms requires the location of the different stationary points such as minima associated with reactants, products, and possible intermediates and saddle points associated with the transition structure (TS) on the potential energy surface (PES). Exploration of PESs with a very high dimensionality has become very recently affordable.[17] This is a crucial step to know the molecular details of chemical reactions occurring in enzymatic media. In a previous study we reported the results of a combined classical/quantum modeling study for the reduction of 5,6-dihydrofolate catalyzed by ecDHFR, the key point being the characterization of the TS associated with the hydride transfer from the cofactor (nicotinamide adenine dinucleotide phosphate, NADPH).[18] In the present paper, we report the results of the previous step, the proton transfer, presumably from Asp27 to the N5 atom of the substrate. This global transfer process from Asp27 to N5 implies

10.1021/jp0354898 CCC: $25.00
Published on Web 11/21/2003

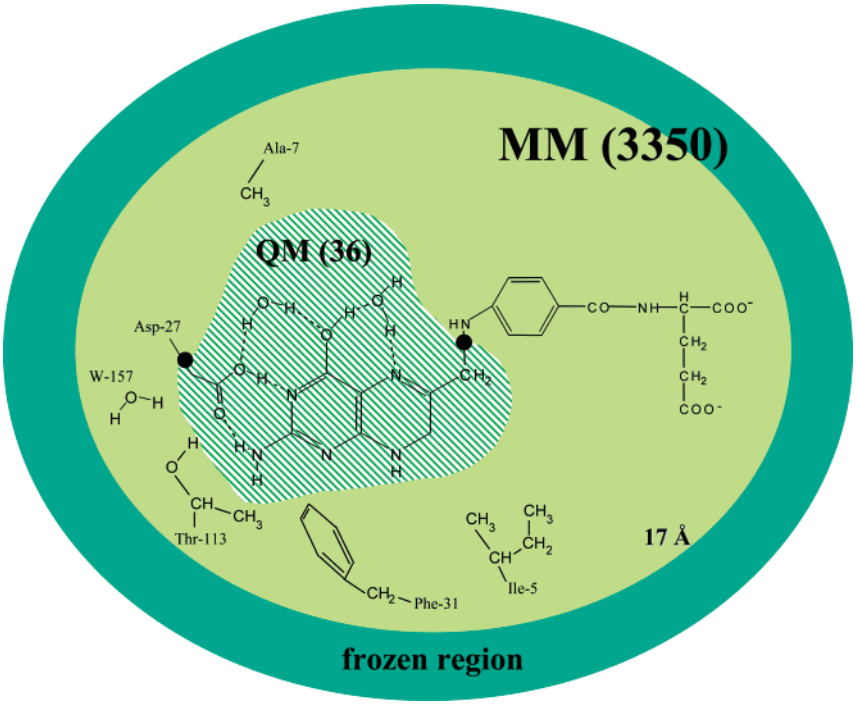

Figure 1. Schematic pictorial of the QM/MM model. Hydrogen quantum link atoms, indicated as dots "•", divide the quantum (shaded area) and classical (solid color areas) regions. The darkest gray region contains the classical described atoms that were frozen during the optimizations.

SCHEME 1

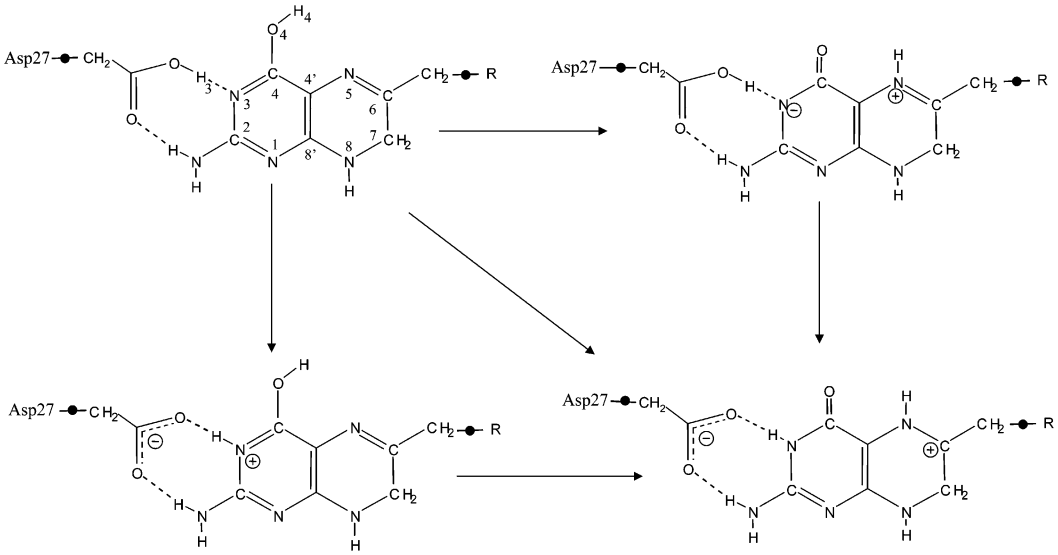

two different proton transfers: from Asp27 to the N3 atom of the substrate and from the enol oxygen (O4) to N5. These two transfers can take place either at the same time or in a stepwise manner, which would render two different paths depending on the order in which the two transfers occur. Thus, in principle, up to three different routes would be possible, as shown in Scheme 1.

Computational Details

The QM/MM energy hypersurface was obtained using the CHARMM24 program[19] as described previously for reactions in aqueous solution[20] and in solvated enzyme active sites.[17,20,21] The starting geometry comes from the 1.6 Å resolution ternary complex X-ray crystal structure of an Escherichia Coli DHFR (ecDHFR−NADPH−Folate).[22] CHARMM24 was also used to add hydrogens to all titratable residues at a state complementary to pH 7. The system was placed in a cavity deleted from a preformed 17 Å radius sphere of TIP3P[23] water molecules centered on the N5 nitrogen atom. Once the entire system was built, those atoms 17 Å away from the active site were frozen during the optimizations to maintain the water sphere and crystal structure. The resulting model, depicted in Figure 1, was a pseudosphere of 3385 atoms, 608 of them kept frozen. The full system was divided into a QM region (36 atoms consisting on the same atoms used for the model in gas phase plus an extra mater molecule), treated by the AM1 semiempirical MO method, and a MM region comprising the rest of the protein (CHARMM24 potentials) and the water molecules. Of course, it would be ideal to use higher level methods, because semiempirical Hamiltonians can be problematic for describing bond breaking/forming processes. However, this is computationally impractical because our calculations typically involve

SCHEME 2

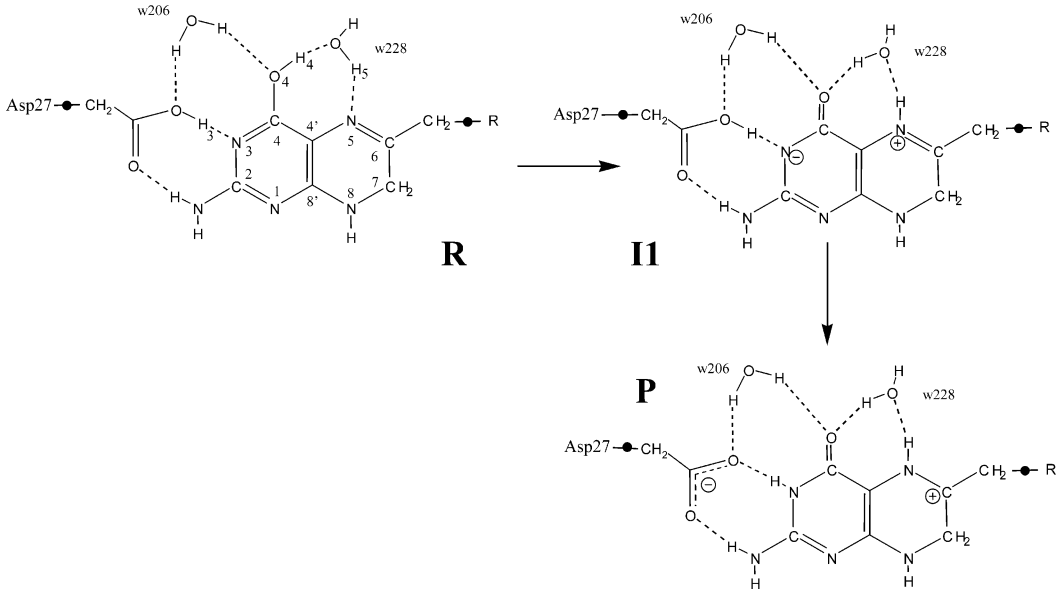

thousands of optimization steps and the evaluation of a large Hessian matrix several times along the stationary point search. Two hydrogen "link atoms",[24] where covalent bonds cross the boundary between the QM and the MM regions, were added to satisfy the valence of the QM fragments. The structural formula of O4 protonated DHF (DHF) is depicted in Figure 1, where the quantum link atoms are indicated as "•".

In the initial complex we placed the substrate in the product state. This structure was fully relaxed and then several scanning grids were used for the initial step of the PES generation. Once the final PESs were obtained, localized approximate TSs were refined using the GRACE software.[17] A partitioned rational function optimizer combined with an adopted-basis-Newton−Raphson method was employed, utilizing a finite-difference Hessian matrix of order 108, describing the curvature of the QM/MM energy hypersurface for the quantum region subset of the system, together with a diagonal Hessian plus updates for the rest of the system. The rms residual gradient on the 36 atoms in the subset has been imposed to be less than 0.1 kcal/mol $Å^{-1}$ in the optimized structure, whereas on the remaining atoms (ca. 3000) it is less than 0.005 kcal/mol $Å^{-1}$; these residual gradients are lower than the commonly accepted convergence criterion for optimized geometries of small molecules in quantum chemistry.[25] Finally, intrinsic reaction coordinate (IRC)[26] paths were traced from the TSs in each direction to demonstrate conclusively that the reported structures are indeed the TS for the correct step under study.

Finally, once the QM/MM potential energy profiles were obtained, the correction of the zero point vibrational energy was estimated for the subset of atoms included in the Hessian calculation. Again, AM1 presents some limitations as this method already contains zero point energies in its parametrization and then some contributions could be double counted. However, the neglect of the zero-point energy variation associated with the imaginary-frequency mode can lead to larger errors and then it may be preferable to include this term explicitly in the calculations.[27]

Results and Discussion

From the exploration of the AM1/MM PES we obtained two possible reaction paths. These two paths correspond to two possible stepwise routes: (1) a proton transfer from enol O4 atom to N5 followed by the proton transfer from Asp27 to N3 and (2) a proton transfer from Asp27 to N3 followed by the transfer from O4 to N5 (this last transfer has been found to take place in two steps with the formation of an additional intermediate). The first path corresponds to the R → I1 → P process (Scheme 2) through TS1 and TS2 transition structures and the second one to the R → I2 → I3→ P process (Scheme 3) through TS3, TS4, and TS5 transition structures. It is important to stress on the nature of the I3 structure: although, a priori, the step from I2 to P in path 2 could be expected to take place as a single step, we located a stationary structure where the H4 proton transfer is not coupled with the H5 proton transfer. A protonated water 228 is stabilized by the environment thus obtaining a new local minimum, I3 (see Scheme 3). Total and relative energies to R, obtained with the AM1/MM calculations, are reported in Tables 1 and 2 for paths 1 and 2, respectively. We also present some selected interatomic distances for all the stationary point structures and the imaginary frequencies characteristic of the transition structures. From an energetic point of view, a first insight into Tables 1 and 2, or the resulting energy profiles depicted in Figure 2, allows us to conclude that the global process is an exothermic reaction (−5.9 kcal/mol). Thus, the enzymatic environment stabilizes the final products when compared to gas-phase calculations.[28] From the kinetic point of view, the two mechanisms are competitive with activation energies of around 23 kcal/mol. It must be kept in mind that these results are obtained with a semiempirical description of the quantum region of our QM/MM model and thus nonnegligible errors could affect the predictions about the activation energies.

As can be seen in Tables 1 and 2, the crystal water molecules seem to remain in ordered positions during the reaction. In this regard (see the O_w−X columns), water 228 acts as a proton relay accepting a proton (H4) from O4 and transferring a proton (H5) to N5 (see Schemes 2 and 3). These events take place concertedly (R → I1 step in path 1) or by steps (I2 → I3 → P steps in path 2), but in all cases product P is hydrogen bonded, by the w228 molecule, to N5 and O4. The difference is that although w228 is acting as proton acceptor with respect to O4 and proton donor to N5 in R, we found the opposite situation; proton donor to O4 and proton acceptor from N5, in P. On the other hand, though w206 remains at H-bond distances from O4

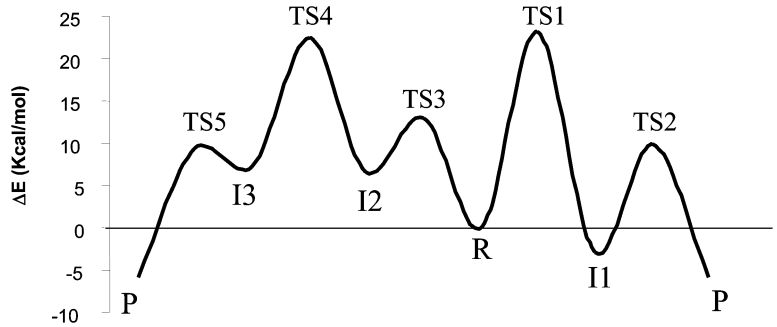

Figure 2. Potential energy profiles for the two located and characterized molecular mechanisms, path 1 (R to TS1 to I1 to TS2 to P) and path 2 (R to TS3 to I2 to TS4 to I3 to TS5 to P), obtained by means of QM/MM calculations.

SCHEME 3

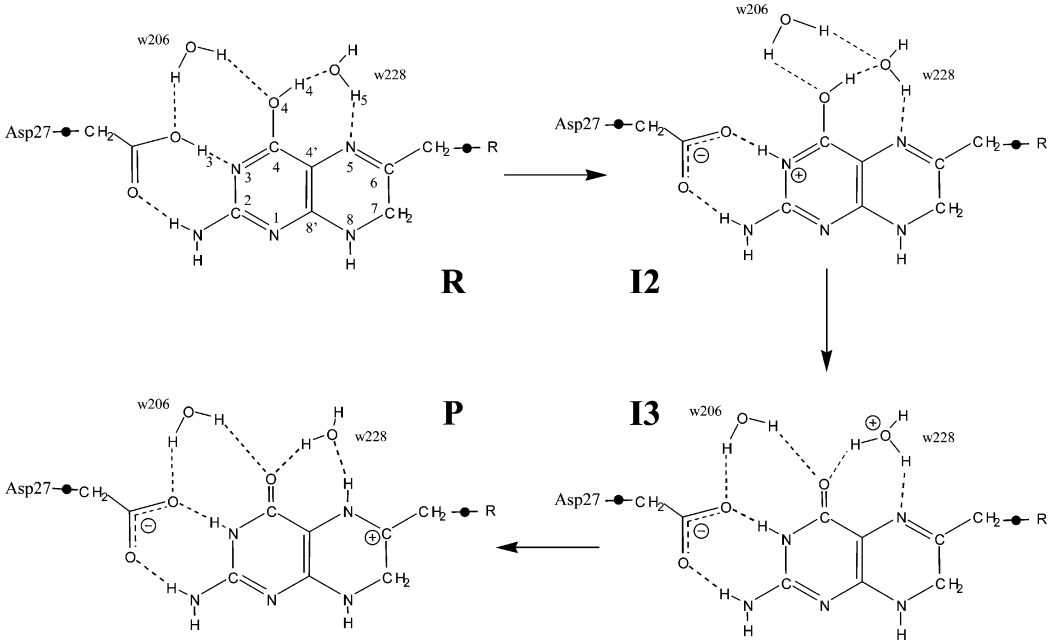

TABLE 1: QM/MM Reaction Path 1, Total Energy and Relative Energy to R (kcal/mol) and Selected Interatomic Distances (Å) for All the Stationary Point Structures, and Imaginary Frequencies (cm^{-1}) Characteristic of TS1 and TS2

			distances (Å)					
	energy (kcal/mol)	ΔE	d(O4−H4)	d(Ow−H4)	d(Ow−H5)	d(N5−H5)	d(N3−H3)	ν (cm^{-1})
R	−6547.1	0.0	0.98	1.96	0.97	2.84	2.36	
TS1	−6524.0	23.2	1.44	1.11	0.99	2.65	2.21	660i
I1	−6550.0	−2.8	3.6	0.96	2.04	1.03	2.22	
TS2	−6537.3	9.9	3.36	0.96	2.03	1.03	1.29	1279i
P	−6553.1	−5.9	3.24	0.96	2.01	1.03	1.02	

TABLE 2: QMM Reaction Path 2, Total Energy and Relative Energy to R (kcal/mol), Selected Interatomic Distances (Å) for All the Stationary Point Structures, and Imaginary Frequencies (cm^{-1}) Characteristic of TS4, TS5, and TS6

			distances (Å)					
	energy (kcal/mol)	ΔE	d(O4−H4)	d(Ow−H4)	d(Ow−H5)	d(N5−H5)	d(N3−H3)	ν (cm^{-1})
R	−6547.1	0.0	0.98	1.96	0.97	2.84	2.36	
TS4	−6534.2	13.0	0.98	1.94	0.97	2.89	1.20	1223i
I2	−6540.5	6.6	0.98	1.92	0.97	2.93	1.02	
TS5	−6524.8	22.4	1.26	1.29	0.99	2.64	1.01	827i
I3	−6539.9	7.2	2.18	1.02	1.02	2.82	1.01	
TS6	−6537.8	9.3	2.50	1.00	1.21	1.35	1.01	924i
P	−6553.1	−5.9	3.24	0.96	2.01	1.03	1.02	

in all minima energy structures on the PESs (2.53, 2.28, 2.67, 2.21, and 2.20 Å for R, I1, I2, I3, and P, respectively) its H-bond interaction with Asp27 is a common feature for all structures but for the I2 intermediate (2.67, 2.45, 2.05, and 2.64 Å for R, I1, I3, and P, respectively). In this case, the H-bond is broken and a new w206−w228 interaction is formed. So, it could be hypothesized that the w206 water molecule would be responsible of the prior step required to arrive at R in which the O4 had been enolized; H4 would be originally bonded to water 206 and one of its hydrogen atoms bonded to Asp27 (the one H-bonded to Asp27 in R). After this process takes place, a rotation of H4 around the C4O4 bond and w206 reorientation

TABLE 3: Selected Substrate−Enzyme Interatomic Distances (Å) for All the Stationary Point Structures Obtained from the QM/MM Calculations

	R	I1	I2	I3	P
O(ILE5):H8(DHF)	1.86	1.87	1.84	1.86	1.81
O(w157):H91(DHF)	1.99	2.03	1.99	2.00	1.97
H61(THR113):OD2(ASP)	1.95	1.94	1.85	1.95	1.84
HD1(PHE31):N1(DHF)	2.69	2.68	2.70	2.70	2.71
HG12(ILE5):N8(DHF)	3.32	3.39	3.42	3.31	3.41
HB2(ALA7):N3(DHF)	2.71	2.73	2.78	2.72	2.86

would be required to reach the R structure. Therefore, both w206 and w228 play a direct role in the network of waters, which helps to the global transfer of a proton from Asp27 to the N5−C6 bond, as suggested previously by Cannon and co-workers.[6] Nevertheless, a note of caution must be considered as these conclusions come from QM/MM potential energy calculations and not from dynamical exploration of a large number of structures. Calculation of free energies would also provide information related with entropic effects, which could be quite important for the proton relay mechanism.

With respect to the active site residues, as can be observed in Table 3, most of the distances between the protein and the substrate remain constant on going from R to P. These results could be interpreted as evidence of the small reorganization of the enzymatic surroundings during the chemical reaction. The fact that the structure of the enzyme does not change dramatically during the reaction has been also observed in other enzymatic systems,[29,30] but usually associated with single-step processes. In other cases, when the enzyme catalyzes multistep chemical processes, the enzyme flexibility can be very important to adapt the active site to the reaction requirements. This is, for example, the case of β-lactamases where some residues can suffer important displacements, allowing them to play an active role even if they were initially located far away from the substrate.[31] With respect to our system, molecular dynamics simulations performed on three ternary complexes from the DHFR catalytic cycle by Brooks and co-workers[32] suggest the importance of correlated motions and structural perturbations. Although they observed that the protein maintained a core structure similar to the initial X-ray model, several loop conformational changes caused dramatic differences in the behavior of the protein dynamics. More recent calculations carried out by Hammes-Schiffer and co-workers,[33] based on hybrid quantum-classical molecular dynamics simulations and empirical valence bond (EVB) potentials,[34] for diverse wild-type DHFR species and mutants, suggest enzyme reorganization is significant for the following step; the hydride transfer reaction (the rate-limiting step). Motions of residues both in the active site and distal to the active site impact the free energy of activation and the degree of barrier recrossing for this chemical step.

The analysis of the normal-mode frequencies of the TSs yields relatively high imaginary frequencies (see Tables 1 and 2), associated with forming/breaking bonds. The dominant amplitudes of these vectors are related to the interatomic distances of donor and acceptor atoms in each step. Other normal modes, corresponding to the second, third, etc. eigenvalues are significant smaller (ca. 60 cm^{-1}), revealing quite soft movements. It can be considered that the active site helps the system in softening the vibrational degrees of freedom, as also shown in previous related works[18,35] where comparative analysis of vacuum versus enzyme QM/MM studies were carried out.

In addition to the analysis of the geometrical aspects, it is also interesting to study the reaction from an electronic point of view. For this purpose we have used the Mulliken charges summed for different subfragments of the reaction system[34] (the Asp27 residue, and the pyrazine and pyrimidine rings). Of course, the absolute value of these charges can be unreliable and other methods would be preferable, but the variation along a reaction path can give a reasonable picture of the electronic evolution of the process. According to this, the reaction can be viewed as a partial electron transfer from pyrazine and pyrimidine rings toward Asp27, thus preparing the system for the subsequent hydride transfer to C6. The calculations describe a neutral Asp27 in R, whereas its total charge in P is −0.96 au. The pyrazine ring follows the opposite trend: 0.03 au in R and 0.68 au in P. This is a very interesting result considering the fact that the C6, as mentioned above, is accepting a hydride anion in the following step. It must be here remembered that this hydride transfer is the rate-limiting step for the global process of DHF reduction to THF by DHFR. This electronic analysis also reveal the electrostatic stabilization of the protonated substrate by Asp 27, as pointed out by Callender et al. on the basis of their Raman studies.[12]

Conclusions

In this paper we present a theoretical study of the chemical reaction step prior to the hydride transfer in dihydrofolate reductase. The employed hybrid quantum-mechanical/molecular-mechanical (AM1/CHARMM24/TIP3P) technique has allowed us to include the protein environment and to explore structural features of significance on hypersurfaces spanning several thousand degrees of freedom. We have focused our interest in the stationary points on the PES, which have been located and characterized involving a fully flexible active-site region by means of GRACE software. Theoretical predictions have been compared with previous published experimental data. The analysis of the results can be summarized as follows.

We have explored two possible reaction paths for the activation of the substrate to proceed for the next step, the hydride transfer step. Both routes, which appear to be energetically competitive, explain the protonated state of the Asp27 and its role in stabilizing the cationic pyrazine ring. Furthermore, our calculations reveal the active role of the water molecules that have been detected in all DHFR crystal structures. The ordered structure of the X-ray crystallographic water molecules support the hypothesis of an indirect transfer of a proton from Asp27 residue to the N5 atom of the substrate. We have found that w206 serves to stabilize Asp27 whereas w228, together with the aforementioned w206, serve as a channel of hydrogen atoms from the Asp27 to the N5 of the pterin ring.

Acknowledgment. We are indebted to DGI for project DGI BQU2000-1425, BANCAIXA for project P1A99-03, and Generalitat Valenciana for project GV01-324, which supported this research, and the Serveis d'Informàtica of the Universitat de Valencia and the Universitat Jaume I and for providing us with computer capabilities. S.F. thanks DGI for a Ministerio de Ciencia y Tecnología for a doctoral fellowship. E.S. thanks Prof. E. Longo for his hospitality and helpful discussions.

References and Notes

(1) Blakley, R. L. *Folates and Pterins*; Wiley: New York, 1984.

(2) Fierke, C. A.; Johnson, K. A.; Benkovic, S. J. *Biochemistry* **1987**, *26*, 4085.

(3) Kraut, J.; Matthews, D. A. In *Biological Macromolecules and Assemblies*; Jurnak, F. A., McPherson, A., Eds.; Wiley: New York, 1987.

(4) (a) Cummins, P. L.; Ramnarayan, K.; Singh, U. C.; Gready, J. E. *J. Am. Chem. Soc.* **1991**, *113*, 8247. (b) Cummins, P. L.; Greatbanks, S. O.; Rendell, A. P.; Gready, J. E. *J. Phys. Chem. B* **2002**, *106*, 9934.

(5) Howell, E. E.; Villafranca, J. E.; Warren, M. S.; Oatley, S. J.; Kraut, J. *Science* **1986**, *231*, 1123.

(6) Cannon, W. R.; Garrison, B. J.; Benkovic, J. *J. Am. Chem. Soc.* **1997**, *119*, 2386.

(7) Howell, E. E.; Warren, M. S.; Booth, C. L. J.; Villafranca, J. E.; Kraut, J. *Biochemistry* **1987**, *26*, 8591.

(8) Morrison, J. F.; Stone, S. R. *Biochemistry* **1988**, *27*, 5499.

(9) Uchimaru, T.; Tsuzuki, S.; Tanabe, K.; Benkovic, J.; Furukawa, K.; Taita, K. *Biochem. Biophys. Res. Commun.* **1989**, *161*, 64.

(10) Bystroff, C.; Oatley, S. J.; Kraut, J. *Biochemistry* **1990**, *29*, 3263.

(11) McTigue, M. A.; Davies, I., J. F.; Kaufman, B. T.; Kraut, J. *Biochemistry* **1992**, *31*, 7264.

(12) Chen, Y.; Kraut, J.; Callender, R. *Biophys. J.* **1997**, *72*, 936.

(13) Gready, J. E. *Biochemistry* **1985**, *24*, 4761.

(14) Gready, J. E.; Cummins, P. L.; Wormell, P. *Adv. Exptl. Med. Biol.* **1993**, *338*, 487.

(15) Ivery, M. T. G.; Gready, J. E. *Biochemistry* **1995**, *34*, 3724.

(16) Jeong, S. S.; Gready, J. E. *Biochemistry* **1995**, *34*, 3734.

(17) A good example of this kind of methodologies can be found in the following references: (a) Turner, A. J. Doctoral Thesis, University of Bath, 1997. (b) Moliner, V.; Turner, A. J.; Williams, I. H. *J. Chem. Soc. Chem. Comun.* **1997**, 1271. (c) Turner, A. J.; Moliner, V.; Williams, I. H. *J. Phys. Chem. Chem. Phys.* **1999**, *1*, 1323.

(18) Castillo, R.; Andrés, J.; Moliner, V. *J. Am. Chem. Soc.* **1997**, *119*, 2386.

(19) Brooks, B. R.; Bruccoleri, R. E.; Olafson, B. D.; States, D. J.; Swaminathan, S.; Karplus, M. *J. Comput. Chem.* **1983**, *4*, 187.

(20) Barnes, J. A.; Williams, I. H. *J. Chem. Soc., Chem. Commun.* **1996**, 193.

(21) Barnes, J. A.; Williams, I. H. *Biochem. Soc. Trans.* **1996**, *24*, 263.

(22) Sawaya, M. R.; Kraut, J. *Biochemistry* **1997**, *36*, 586.

(23) Jorgensen, W. L.; Chandrasekhar, J.; Madura, J.; Impey, R. W.; Klein, M. L. *J. Chem. Phys.* **1983**, *79*, 926.

(24) Field, M. J.; Bash, P. A.; Karplus, M. *J. Comput. Chem.* **1990**, *11*, 700.

(25) Foresman, J. B.; Frisch, A. E. *Exploring Chemistry with Electronic Structure Methods*; Gaussian, Inc.: Pittsburgh, PA, 1993.

(26) Fukui, K. *J. Phys. Chem.* **1970**, *74*, 4161.

(27) García-Viloca, M.; Alhambra, C.; Truhlar, D. G.; Gao, J. *J. Chem. Phys.* **2001**, *114*, 9953.

(28) AM1 gas-phase calculations of a model system (a molecule of acetic acid that mimics the Asp27, the 6-methyl-substituted pterin that represents the DHF and one water molecule) predict that the reaction is endothermic by about 28 kcal/mol.

(29) Martí, S.; Andrés, J.; Moliner, V.; Silla, E.; Tuñón, I.; Bertrán, J. *Chem. Eur. J.* **2003**, *9*, 984−991.

(30) Torres, R. A.; Schiott, B.; Bruice, T. C. *J. Am. Chem. Soc.* **1999**, *121*, 8164−8173.

(31) Castillo, R.; Silla, E.; Tuñón, I. *J. Am. Chem. Soc.* **2002**, *124*, 1809.

(32) Radkiewicz, J. L.; Brooks, C. L., III. *J. Am. Chem. Soc.* **2000**, *122*, 225−231.

(33) (a) Agarwal, P. K.; Billeter, S. R.; Rajagopalan P. T. R.; Benkovic S. J.; Hammes-Schiffer S. *PNAS* **2002**, *99*, 2794−2799. (b) Agarwal, P. K.; Billeter, S. R.; Hammes-Schiffer S. *J. Phys. Chem. B* **2002**, *106*, 3283−3293. (c) Watney J. B.; Agarwal, P. K.; Hammes-Schiffer S. *J. Am. Chem. Soc.* **2003**, *125*, 3745−3750. (d) Rod T. H.; Radkiewicz, J. L.; Brooks, C. L., III. *Proc. Natl. Acad. Sci.* **2003**, *100*, 6980.

(34) Warshel, A. *Computer Modelling of Chemical Reactions in Enzymes and Solutions*; John Wiley: New York, 1991.

(35) Moliner, V.; Andrés, J.; Oliva, M.; Safont, V. S.; Tapia, O. *Theor. Chem. Acc.* **1999**, *101*, 228.

(36) As pointed out by Alhambra and co-workers (Alhambra, C.; Wu, L.; Zhang, Z.; Gao, J. *J. Am. Chem. Soc.* **1998**, *120*, 3858) in the original implementation of the link-atom approach (see ref 24) electrostatic interactions between the link atom and the rest of the protein atoms were not included in the quantum calculation. This, however, introduces an imbalance in electrostatic interactions in the QM region due to the fact that molecular orbitals are delocalized and such a partition, which excludes some terms in the Fock matrix, results in an unrealistically large partial charges on link atoms and the atoms they are attached to. This deficiency, inherent in CHARMM link-atom treatment, has to be always kept in mind, and conclusions must be discussed with caution unless a correction is taken into account. In this work, because the quantum link atom charges are constant in all the states, no change in the polarization have been induced by the MM charges from R to P. This result means that a minimal artifact result is obtained by the presence of these virtual H atoms in the relative magnitudes, although the total charge on C6 can be polarized by the close presence of the negative charge in the link atom. Due to this reason, we have preferred to calculate and analyze the sum of the charges of the pyrazine ring, which renders a more realistic result. Furthermore, the Mulliken charge analysis approach has been shown to be highly basis set dependent. Nevertheless, considering the rest of the limitations related with the AM1/TIP3P optimization method implemented in CHARMM, the electronic analysis derived from these calculations can be considered qualitatively acceptable.